Supporting Information

Ligand-mediated manganese phosphonates with variable morphological framework: efficient for energy storage application

Rupali Ipsita Mohanty,[a,b] Ayan Mukherjee,[a] Piyali Bhanja,[a,*] Bikash Kumar Jena,[a,b,*]

[a]*Materials Chemistry Department, CSIR-Institute of Minerals and Materials Technology, Bhubaneswar-751013, India*

[b]*Academy of Scientific and Innovative Research (AcSIR), Ghaziabad-201002, India*

Corresponding author: piyalibhanja4@gmail.com, bikash@immt.res.in

1. Instrumentation

Rigaku RINT 2500X diffractometer with monochromated Cu Kα radiation (40 kV, 40 mA) at a scan rate of 0.1° min^{-1} was used to measure the wide-angle powder X-ray diffraction (XRD) patterns for three as-prepared materials. Unit cell structures of these metal phosphonates were generated using EXPO2014 software with built-in Rietveld refinement of the powder XRD data. FT-IR spectra of three samples were analyzed using a Thermo Scientific Nicolet 4700 spectrometer. Quantachrome Autosorb was used for nitrogen sorption analysis of four samples after outgassing the as-synthesized samples at 150 °C for 12 h. The scanning electron microscope (SEM) images of all the materials were obtained from Hitachi SU-8000 SEM, having an accelerating voltage of 15 kV. To analyze the oxidation states of the metal center of the as-prepared four materials, the X-ray photoelectron spectroscopy technique was used with Kratos Axis Ultra XPS. The TEM images and elemental mapping for all samples were taken by an FEI F20 FEG-STEM instrument after drop-casting the sample onto the copper grid.

2. Electrochemical measurements

All the electrochemical measurements were carried out at room temperature by both three-electrode and two-electrode systems using the electrochemical workstation Biologic VSP-300. A three-electrode cell was used for electrochemical measurement in a 1M KOH electrolyte with the prepared sample coated on a glassy carbon working electrode (surface area 0.07 cm^2), Pt wire, and Ag/AgCl as the counter and reference electrodes, respectively. The working electrode was prepared by taking the as-synthesized samples and carbon black (for conductivity) in the ratio 4:1 in 195 µl of absolute ethanol and 5 µl of Nafion solution, followed by ultrasonication for proper dispersion. 10 µl from the resultant solution was drop casted on the glassy carbon electrode and used for electrochemical measurement of the electrode materials.

The two-electrode asymmetric coin cell device was fabricated using our active catalyst MnBPA (2 mg) as positive and commercially available activated carbon (13 mg) as negative material. The mass ratio was calculated according to the equation:

$$m^+/m^- = (C^-. \Delta V^-) / (C^+. \Delta V^+) \quad (1)$$

where m^+ and m^- are the mass of the active material of the positive and negative electrodes, respectively.

C is the specific capacitance value, and ΔV is the potential window.

PVDF membrane was used as a membrane separator and dipped in 1M KOH aqueous electrolyte. All the electrochemical measurements like cyclic voltammetry (CV), galvanostatic charge-discharge (GCD), and electrochemical impedance spectroscopy (EIS) of the two-electrode setup were done using the same instrument Bio-logic VSP-300.

3. Fabrication procedure of MnBPA//AC MSC device

Using a customized mask, the MnBPA material was used to fabricate the micro-supercapacitor device using ultra vacuum filtration on a PVDF membrane substrate. The customized mask possesses eight in-plane interdigital fingers (four per polarity) of 1.8 cm in length, 2 mm in width, and 2 mm in interspace width. First, a 5ml solution of dispersion of MnBPA with carbon black (4:1) and ethanol (0.2 mg/ml) was taken and vacuum filtrated on the PVDF substrate using the mask through four interdigital fingers of one polarity. Carbon black was used to increase the conductivity of the electrode material. After the filtration, a dispersion of commercially available activated carbon with ethanol (2 mg/ml) was vacuum filtrated through another four interdigital fingers of another polarity of the customized mask. PVA/KOH was used as the gel electrolyte, which was prepared by dissolving a 20% PVA solution with 1M KOH solution until the solution became clear. Finally, the MSCs were obtained by dropping the electrolytic solution on the electrodes.

Table S1: Structure of MnBPA

Unit cell= Triclinic

Cell parameter

a=14.4993, b= 9.3543, c= 5.5913 α=96.29, β=95.95, γ= 83.48, V=745.72Å

Space group=1 P 1

h	***k***	***l***	***2θ***	***d***
1	0	0	6.15653	14.34412
1	-1	0	11.89967	7.43100
1	0	-1	16.61567	5.33097
1	0	1	17.68835	5.01002
3	0	0	18.54152	4.78137
0	2	0	19.17786	4.62413
0	1	1	19.47462	4.55433
2	1	-1	20.26296	4.37889
1	-2	0	20.76549	4.27404
2	2	0	21.74730	4.08325
1	2	-1	23.70607	3.75011
2	-2	0	23.93015	3.71550
4	0	0	24.80761	3.58603
1	-2	1	25.48397	3.49237
3	-1	-1	26.66834	3.33989
4	-1	0	27.56896	3.23280
3	-2	0	28.17530	3.16459
4	2	0	29.88681	2.98715
4	0	1	30.91496	2.89010
1	3	-1	31.49505	2.83818
4	-2	0	33.12936	2.70181
5	-1	0	33.62294	2.66327
0	1	2	34.71901	2.58166
2	0	2	35.81672	2.50501
2	-1	2	36.63069	2.45119
5	-1	1	38.30374	2.34789
4	1	-2	38.96724	2.30943
1	2	2	40.22049	2.24031
6	2	0	40.61887	2.21925
6	2	-1	41.75089	2.16166
6	-1	-1	42.21432	2.13899
3	3	-2	43.20107	2.09239
0	4	1	43.87004	2.06203
1	-4	-1	44.72329	2.02465
5	-1	-2	45.88232	1.97616
5	0	2	47.68434	1.90560
3	-3	2	48.50460	1.87528
0	0	3	49.36326	1.84465
6	-3	0	50.63657	1.80121

Table S2: Structure of MnPPA

Unit cell= Tetrahedral

Cell parameter

a= 5.7506, b=28.6314, c=4.9504, α= 90.00, β=90.00, γ= 90.00, V=815.07 Å

Space group= 1 P a

h	***k***	***l***	***2θ***	***d***
0	2	0	6.16877	14.31569
0	4	0	12.35551	7.15784
1	2	0	16.59933	5.33618
1	3	0	17.99416	4.92556
0	6	0	18.57866	4.77190
0	2	1	18.95276	4.67854
0	7	0	21.70992	4.09020
1	0	1	23.69563	3.75174
1	2	1	24.50806	3.62918
0	6	1	25.91228	3.43560
1	7	0	26.72379	3.33309
1	5	1	28.41745	3.13817
1	6	1	30.27901	2.94934
2	0	0	31.07804	2.87531
2	2	0	31.71488	2.81901
1	7	1	32.35358	2.76480
1	8	1	34.60891	2.58962
2	0	1	36.09494	2.48634
2	7	0	38.22995	2.35225
2	5	1	39.47947	2.28063
2	6	1	40.89339	2.20498
2	8	1	44.32428	2.04194
0	9	2	46.44472	1.95353
2	0	2	48.48830	1.87587
1	2	0	49.60801	1.83612
1	4	1	50.80457	1.79564

Table S3: Structure of MnDPA

Unit cell= Triclinic

Cell parameter

a= 15.6495, b=14.8625, c=12.0569, α=103.47, β=96.90, γ= 108.20, V=2533.69 Å

Space group= 0 P 1

h	***k***	***l***	***2θ***	***d***
0	0	1	7.70345	11.46682
1	0	-1	8.76028	10.08570
2	-1	-1	13.56628	6.52162
1	0	-2	15.37040	5.75995
0	0	2	15.44199	5.73341
0	2	-2	17.15535	5.16446
2	1	-2	18.71629	4.73712
2	-3	0	19.14469	4.63207
3	-1	1	19.57639	4.53089
2	-2	2	20.25236	4.38116
3	0	-2	21.37524	4.15348
3	-1	-2	21.76495	4.07998
3	-3	1	22.39092	3.96731
1	3	0	22.59402	3.93211
0	0	3	23.25218	3.82227
1	-1	3	23.76932	3.74027
3	-2	2	24.12304	3.68622
4	0	0	24.46992	3.63475
2	-1	-3	25.44266	3.49794
3	-4	1	26.31715	3.38366
1	3	-3	27.07173	3.29103
4	-2	-2	27.32752	3.26081
3	-4	2	28.60842	3.11766
0	4	-3	29.81261	2.99441
5	-3	1	31.31062	2.85448
1	-3	4	32.31302	2.76818
5	0	1	33.30439	2.68801
0	3	3	34.82405	2.57411
6	-1	-2	36.12445	2.48438
4	0	3	37.50686	2.39592
1	5	1	39.01073	2.30695
4	3	1	39.94349	2.25520
3	4	1	40.61003	2.21971
3	5	-3	42.70379	2.11560
1	3	4	44.41377	2.03804
0	2	-6	45.42704	1.99490
5	-4	-4	46.70099	1.94341
5	-7	-1	48.25271	1.88448
4	4	2	49.95761	1.82408

6	2	2	50.83276	1.79472

Table S4: Structure of MnNAPH

Unit cell= Triclinic

Cell parameter

a= 19.7278, b=10.5028, c=9.3269, α=91.94, β=101.01, γ=90.46, V=1895.68 Å

Space group= 0 P 1

h	***k***	***l***	***2θ***	***d***
1	0	0	8.25628	10.70022
1	-1	0	11.29565	7.82697
1	1	0	12.89688	6.85857
1	-1	1	14.27835	6.19794
0	2	-1	15.77796	5.61207
2	0	0	16.55582	5.35011
2	-1	-1	19.72666	4.49671
1	1	1	20.36337	4.35752
2	0	-2	21.46968	4.13542
2	0	1	22.26489	3.98948
0	3	-1	23.71950	3.74801
3	-1	0	25.36851	3.50800
2	2	-3	27.45477	3.24598
3	-1	1	28.99777	3.07667
1	3	0	29.13871	3.06211
2	0	-3	29.59017	3.01641
0	0	3	30.81772	2.89900
4	1	-2	32.52420	2.75069
2	2	1	32.83404	2.72544
4	-1	-2	35.40347	2.53330
2	3	-4	36.22687	2.47759
1	4	0	38.09620	2.36020
4	3	-2	39.12579	2.30043
4	3	-3	39.57737	2.27522
5	-1	-1	40.66221	2.21698
0	5	-3	41.10048	2.19435
3	1	2	41.81824	2.15833
0	2	3	42.79239	2.11143
5	-2	-1	43.57041	2.07551
2	3	-5	43.81997	2.06427
5	-1	1	45.79295	1.97981
2	-1	4	46.89840	1.93569
4	2	-5	47.65058	1.90687
2	4	1	48.73265	1.86703
2	0	-5	49.20279	1.85029

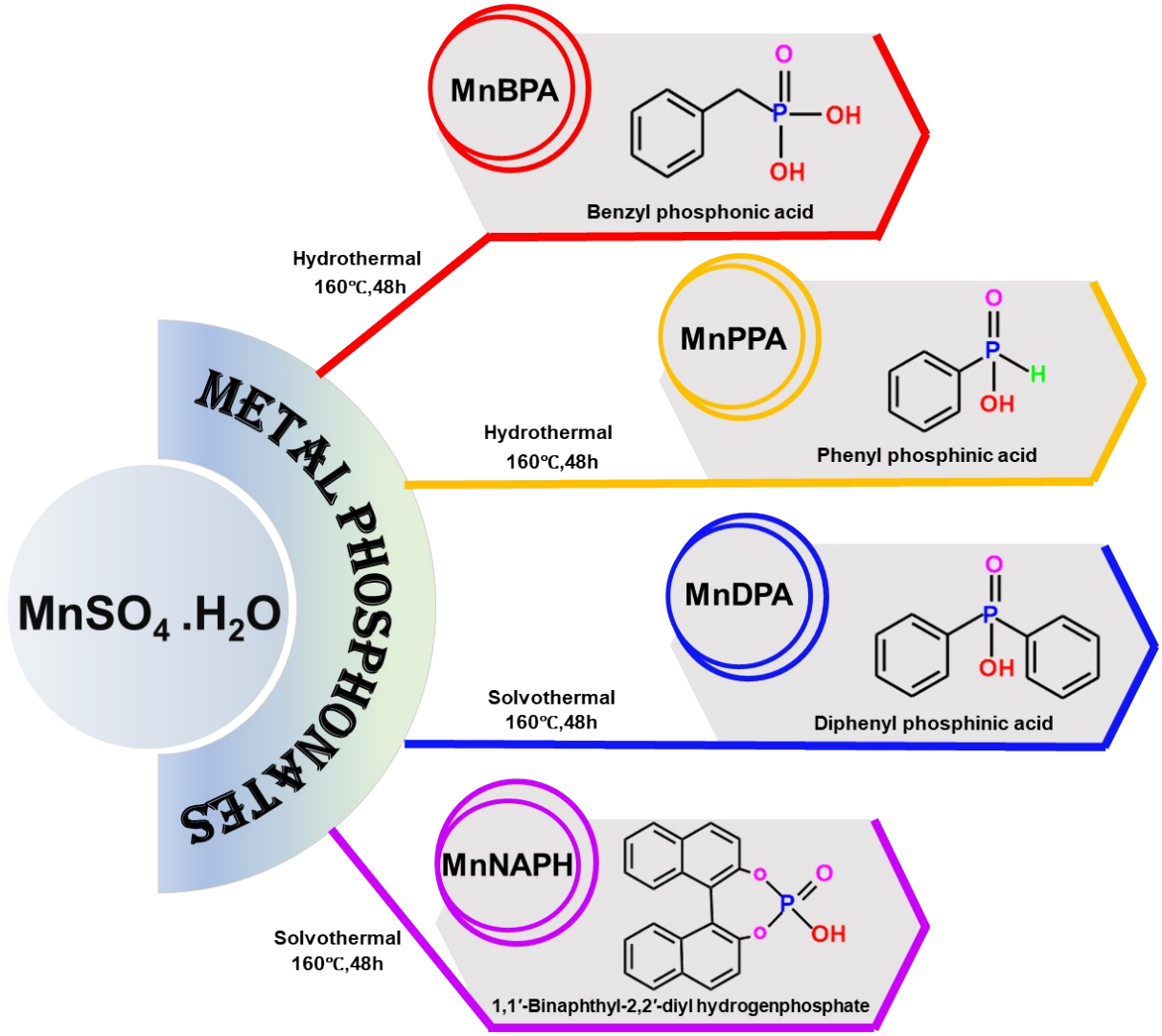

Scheme S1. Schematic representation of the synthesis of manganese phosphonates using distinct organophosphorus ligands.

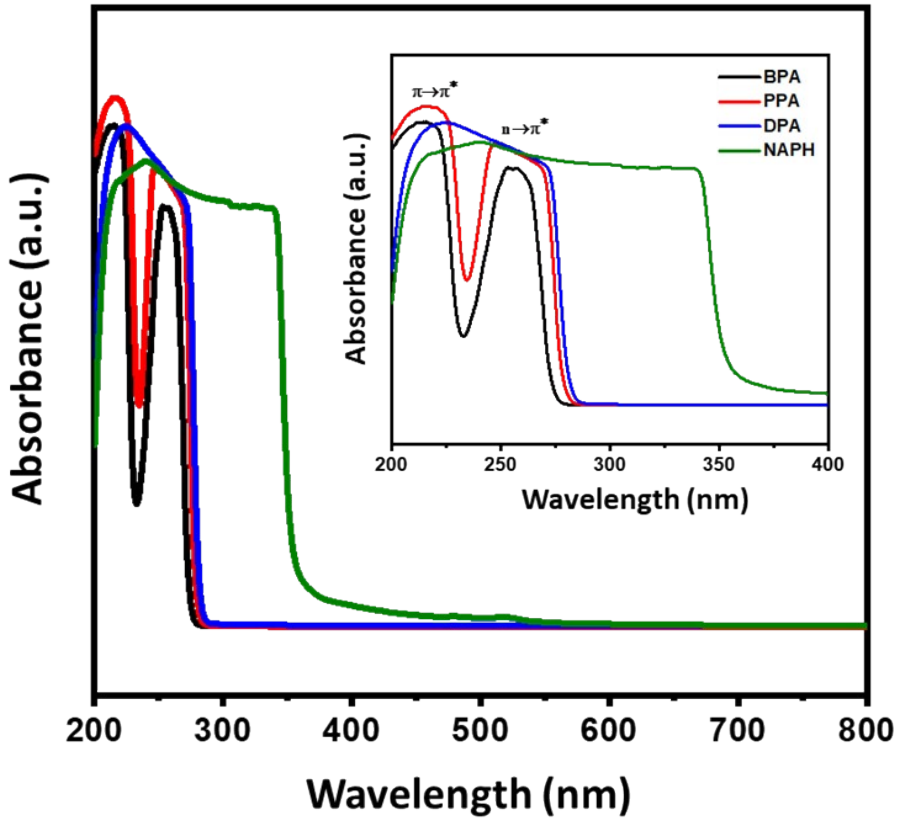

Fig. S1. UV-vis spectra of each aromatic ligand (inset: zoom version of the spectra in the range of wavelength 200-400 nm).

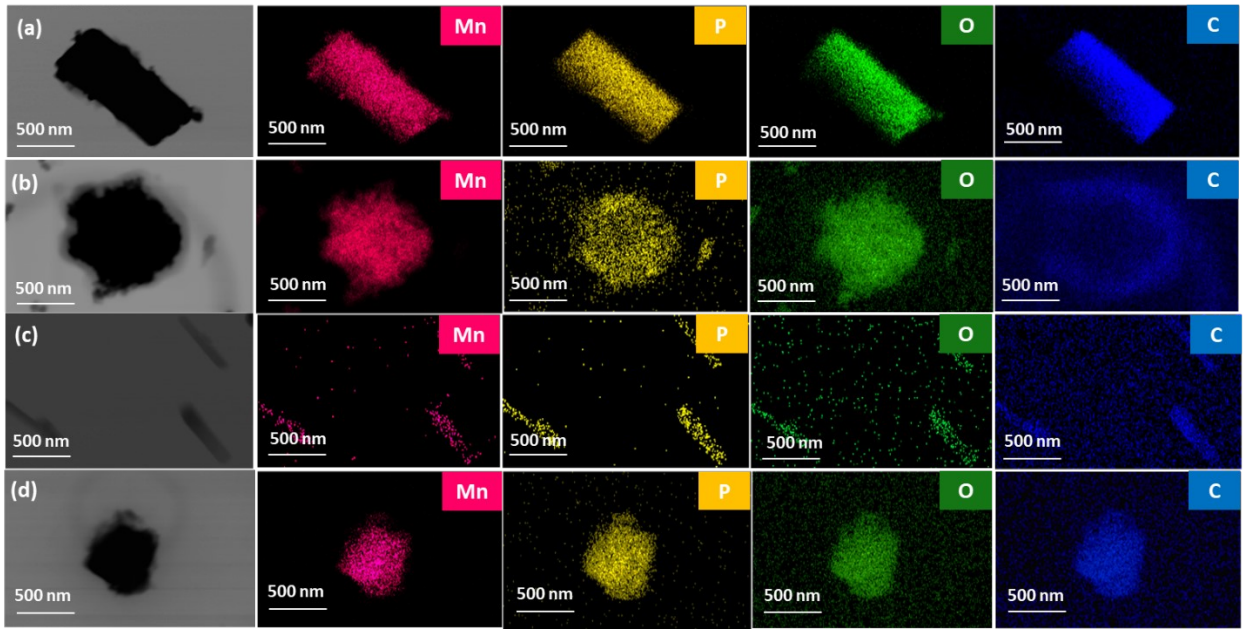

Fig. S2. TEM and the elemental mapping images of (a) MnBPA, (b) MnPPA, (c) MnDPA, and (d) MnNAPH with the desired elements from TEM analysis.

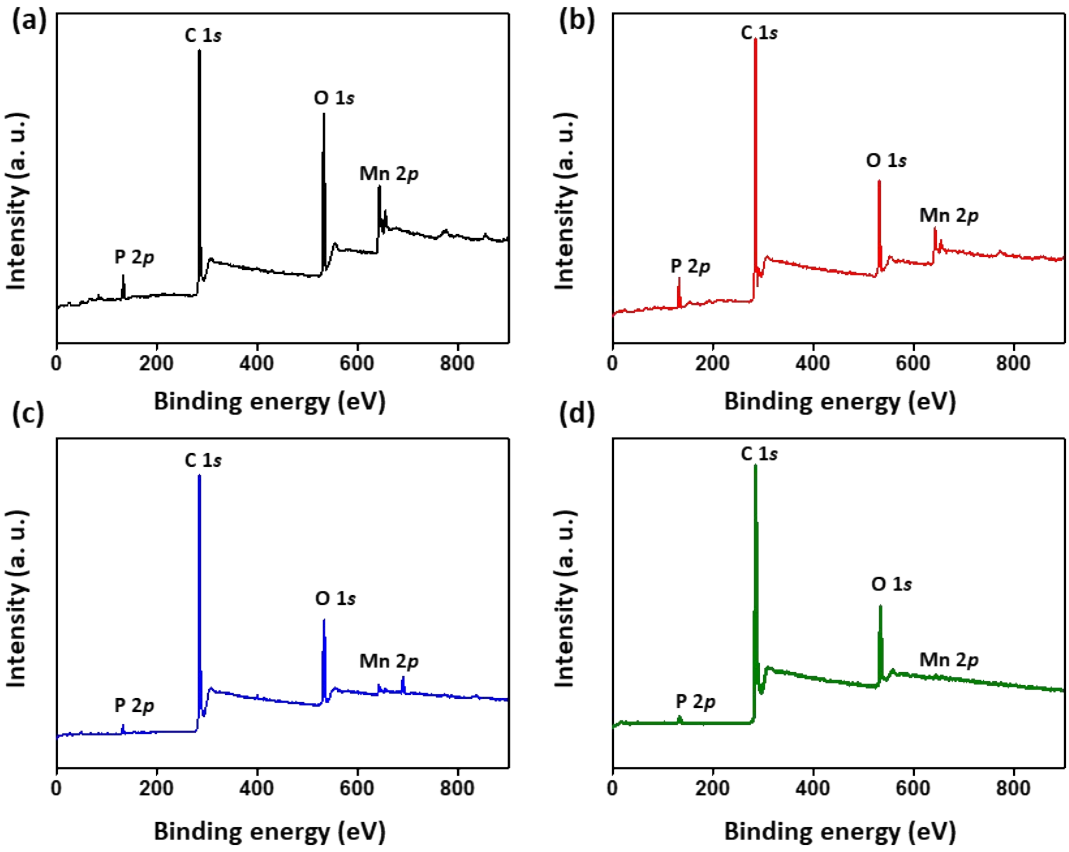

Fig. S3. Full range XPS spectra of (a) MnBPA, (b) MnPPA, (c) MnDPA, and (d) MnNAPH.

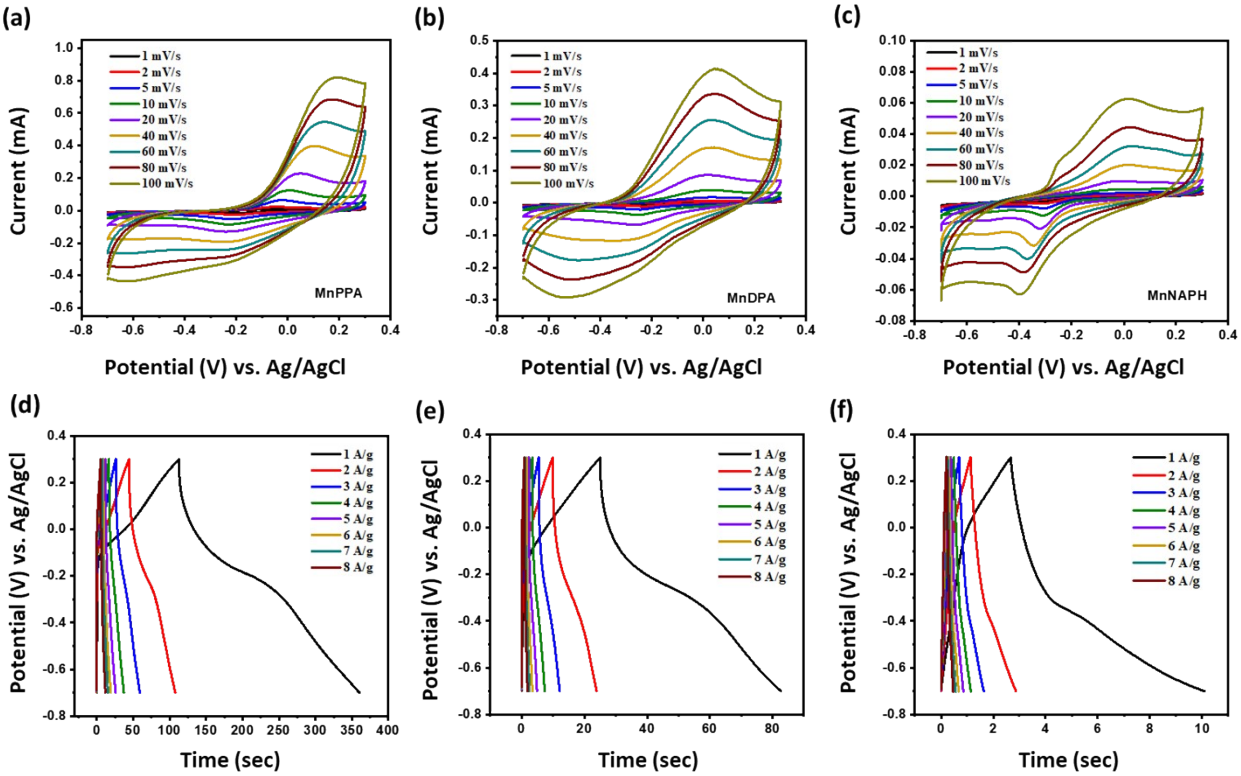

Fig. S4. (a, d) CV and GCD plots of MnPPA, (b, e) CV and GCD of MnDPA, and (c, f) CV and GCD of MnNAPH at different scan rates and current densities.

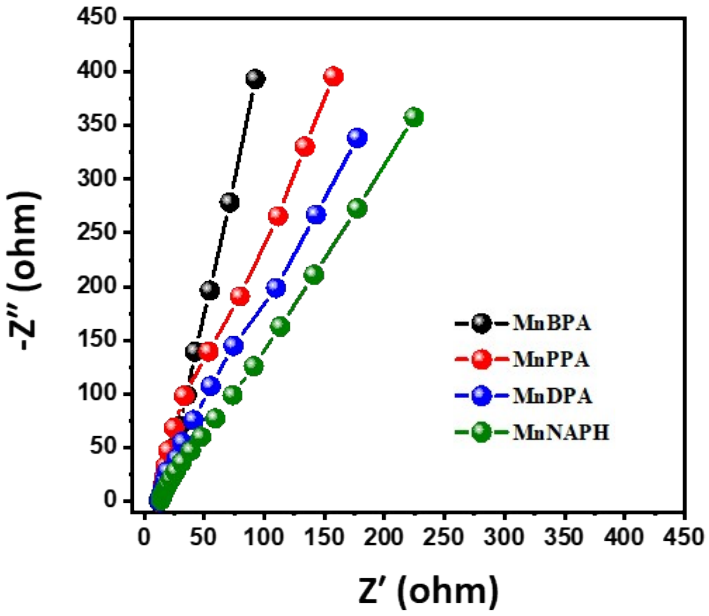

Fig. S5. Comparison EIS spectra of the manganese phosphonates with distinct ligands.

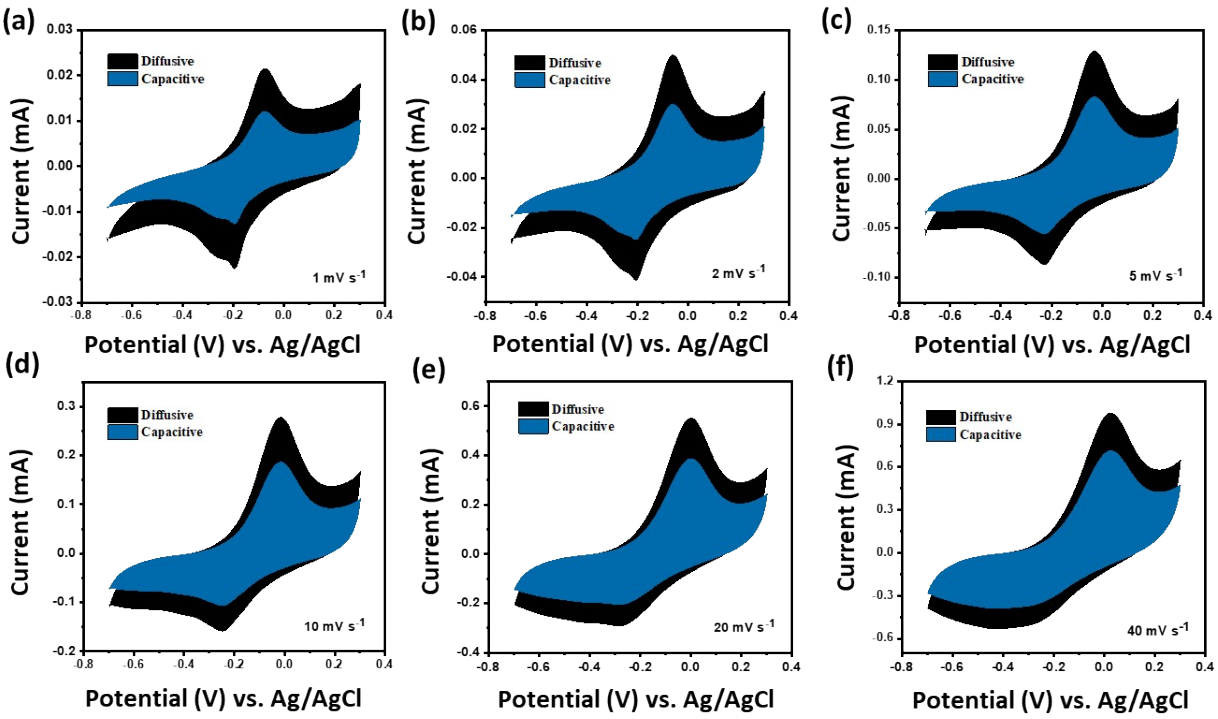

Fig. S6. (a-f) The CV profiles of MnBPA at lower scan rates (1 to 40 mV s^{-1}) with the contribution of diffusion and surface phenomena.

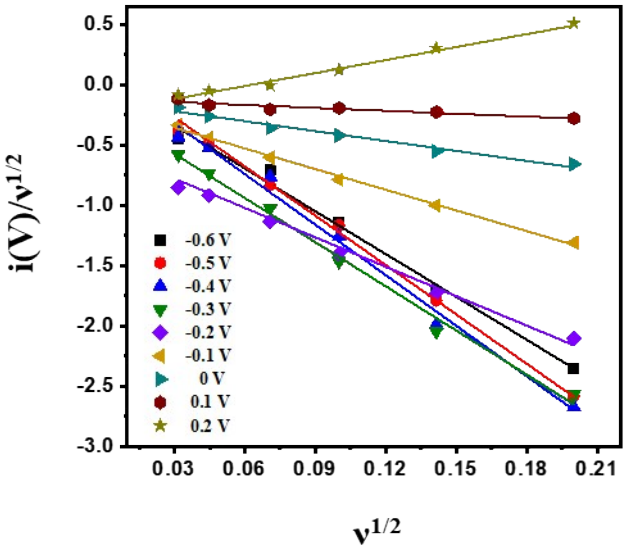

Fig. S7. The plot of i(V)/$v^{1/2}$ vs. $v^{1/2}$ at different potentials for the cathodic region of MnBPA electrode material.

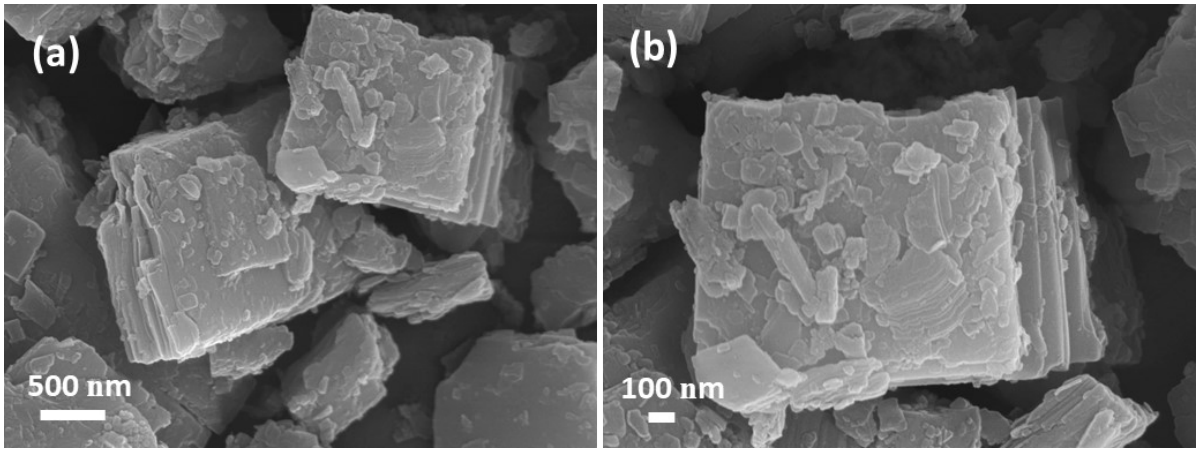

Fig. S8. SEM images of (a,b) MnBPA electrode material after 10000 cyclic stability test in a two-electrode system.

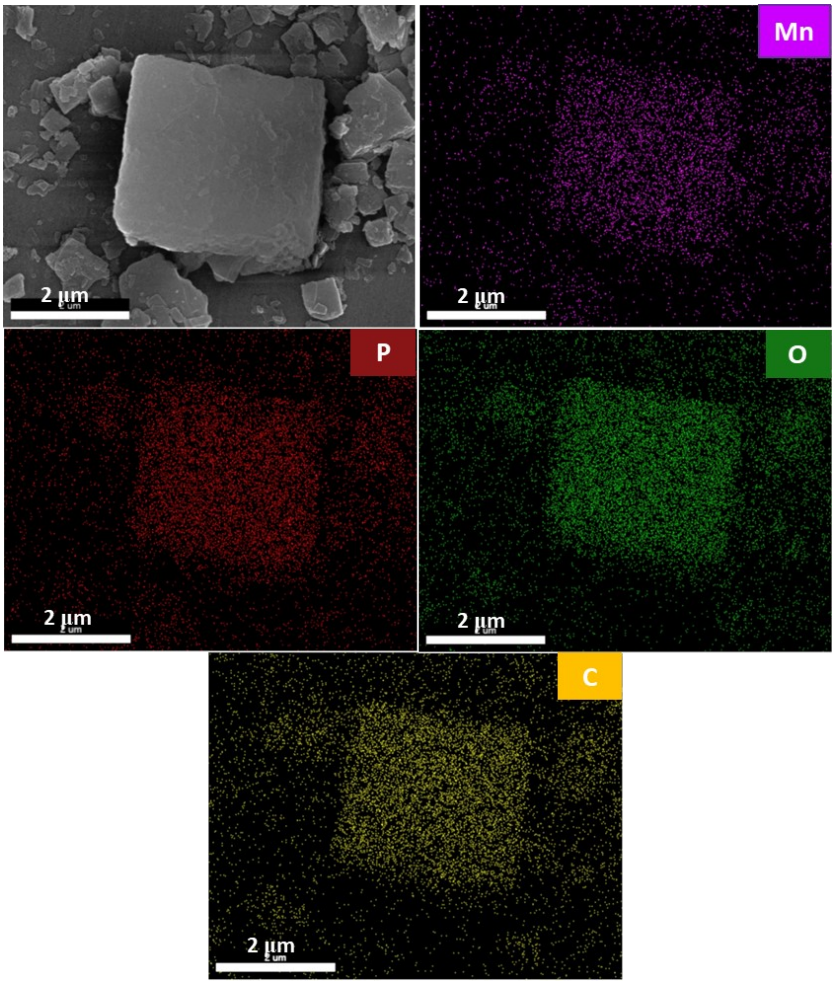

Fig. S9. SEM image and elemental mapping of MnBPA after 10000 cyclic stability test in a two-electrode system.

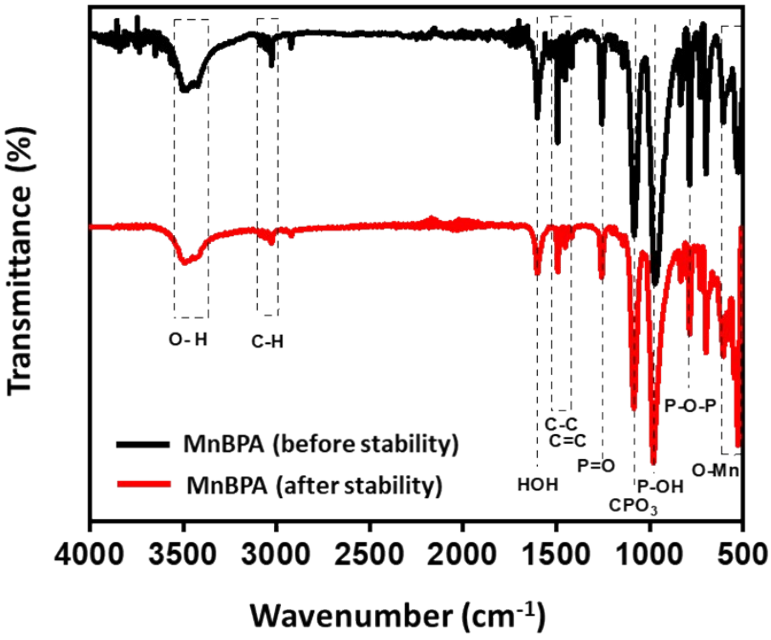

Fig. S10. FTIR spectrum of MnBPA after 10000 cyclic stability test in a two-electrode system.

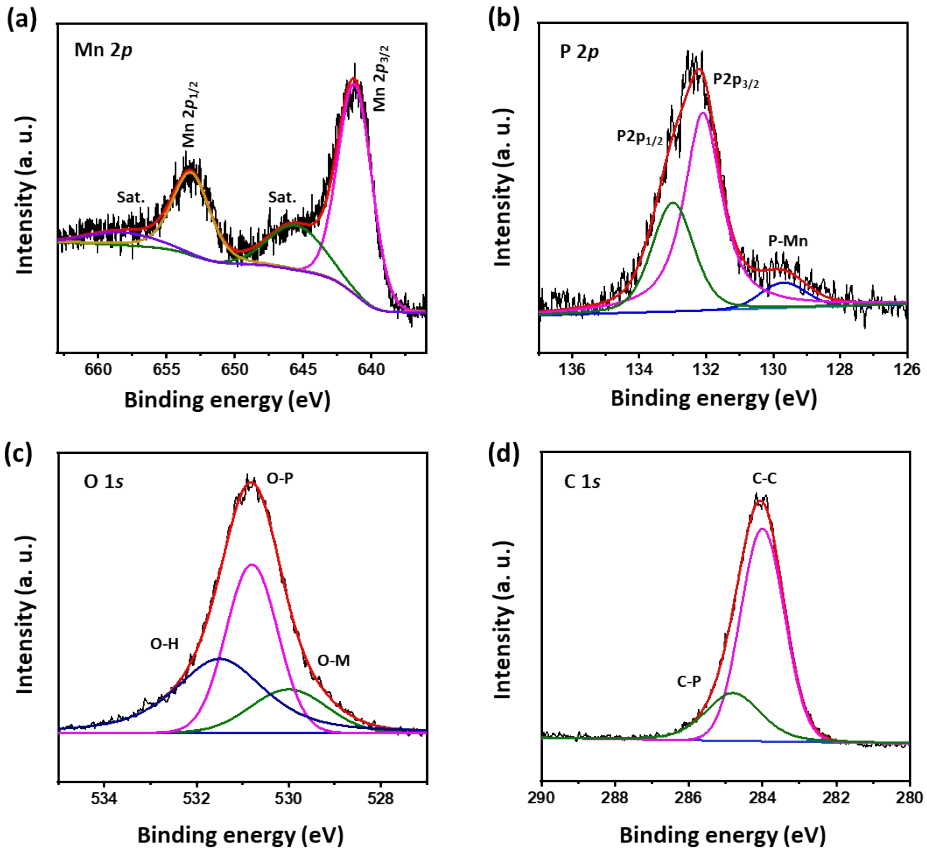

Fig. S11. XPS spectra of (a) Mn 2*p,* (b) P 2*p,* (c) O 1*s*, (d) C 1*s* of MnBPA after 10000 cyclic stability test in a two-electrode system.

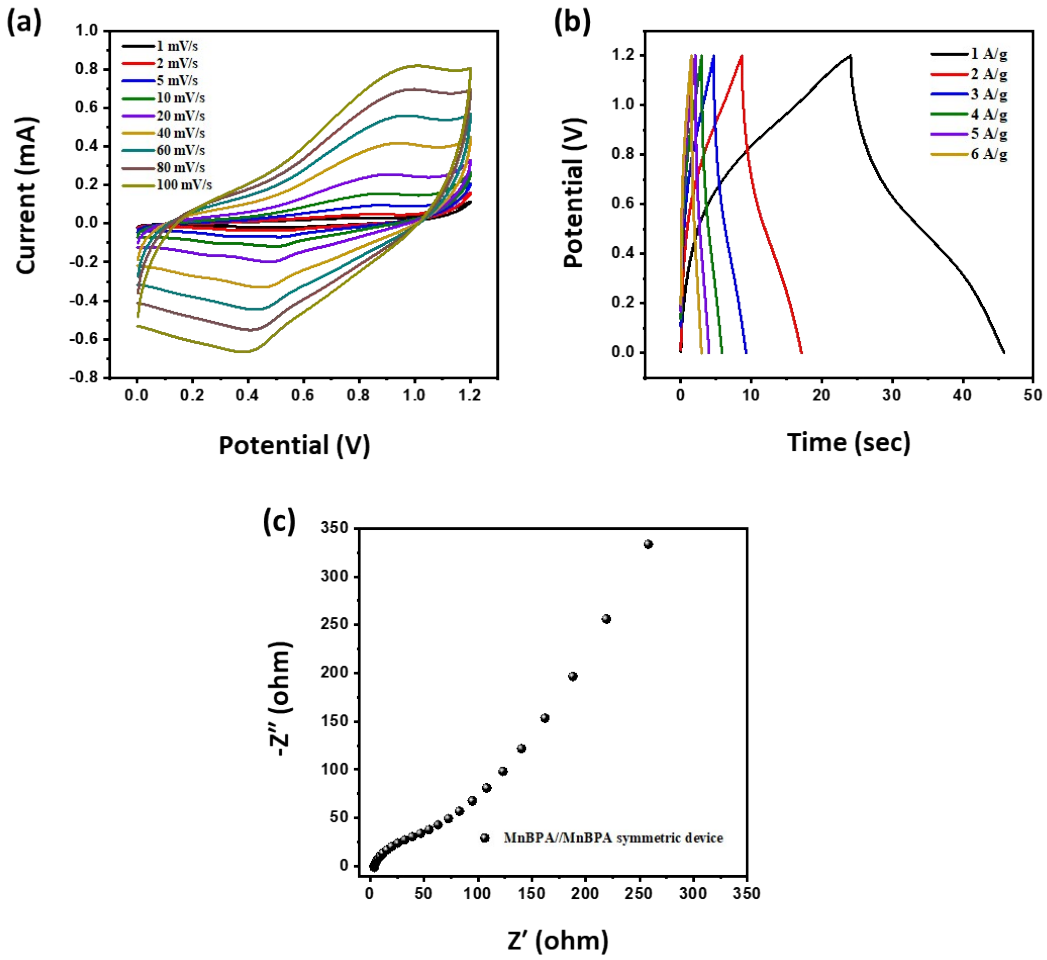

Fig. S12. (a) CV at different scan rates, (b) GCD plot at different current densities, (c) EIS spectrum of MnBPA//MnBPA symmetric device.

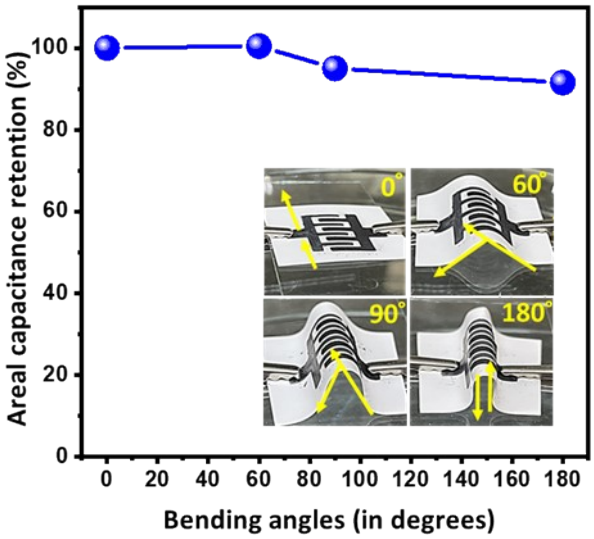

Fig. S13. Areal capacitance retention of the MSC device at different bending angles at 20 mV/s.

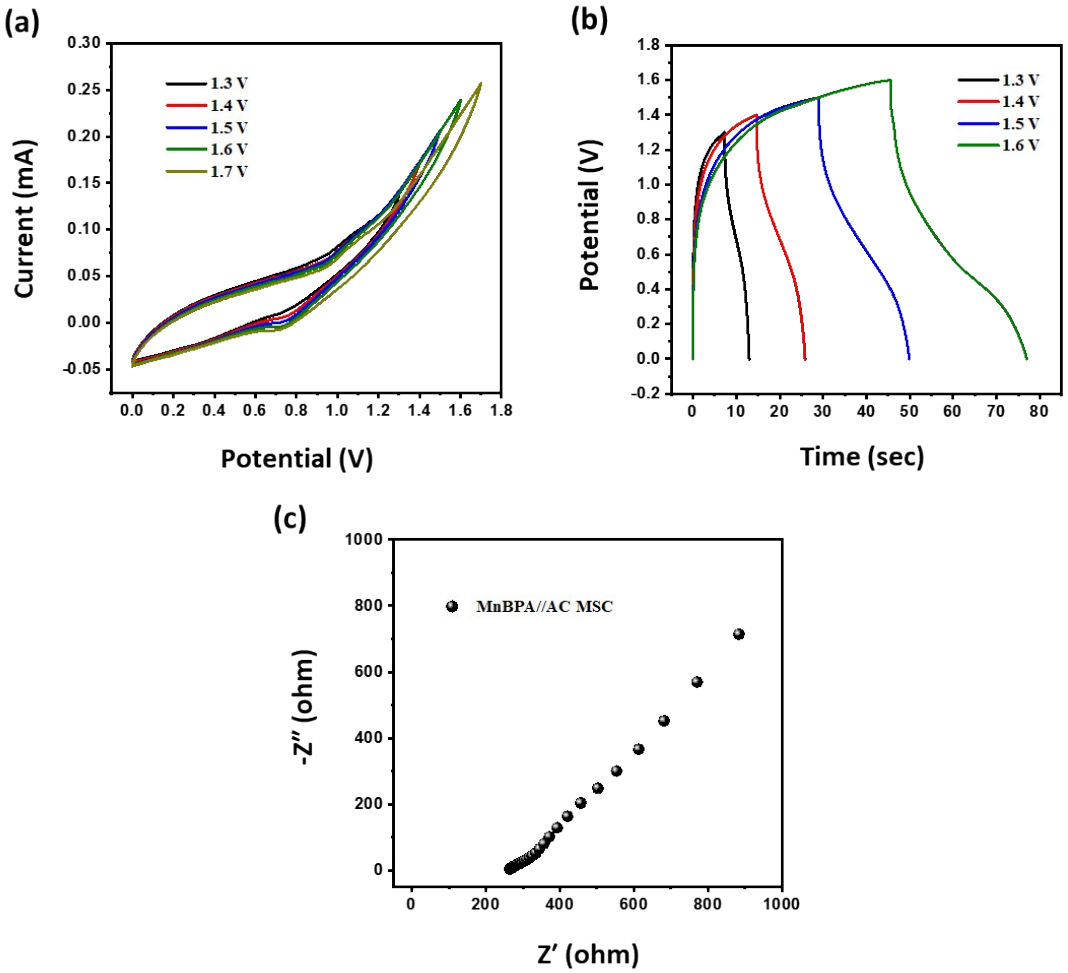

Fig. S14. (a) Step CV, (b) Step CD plots of AMSC device by varying the voltage window, (c) EIS spectrum of MnBPA//AC MSC device.

Table S5. Comparison of energy storage performance of three-electrode system of reported manganese phosphonate and other manganese-based materials with as-synthesized best electrode material MnBPA

Materials	**Specific Capacitance (Fg^{-1})**	**Electrolyte**	**Stability, No. of cycles**	**Reference**
MnOx/GH	352.9 at 1 A g^{-1}	1 M Na_2SO_4	93.8%, 5000	1
MO@CNC-3	435 at 1 A g^{-1}	1 M Na_2SO_4	92.7%, 5000	2
MnO_2	469 at 5 mV s^{-1}	1 M KOH	66%, 5000	3
Mn phosphonate (M-MnP52)	269 at 5 mV s^{-1}	3 M KOH	More than 57%, 1000	4
MnO_2@NAC	408.5 at 0.5 A g^{-1}	6 M KOH	88.2%, 10000	5
$Mn_3(PO_4)_2$/GF	270 at 0.5 A g^{-1}	6 M KOH	99%, 1000	6
Mn_3O_4	273.3 at 0.5 A g^{-1}	6 M KOH	-	7
MnHCF	202.8 at 1 A g^{-1}	1 M Na_2SO_4	95.63%, 8000	8
MnBPA	**846 at 1 mV s^{-1} and 515 at 1 A g^{-1}**	**1 M KOH**	**83%, 1000**	**This work**

Table S6. Comparison of energy storage performance of two-electrode device with reported fabricated device consisting of manganese-based materials

Materials	Specific Capacitance (F g^{-1})	Electro lyte	Stability, No of cycles	Energy density (Wh kg^{-1})	Power density (W kg^{-1})	Refere nces
MnOx/GH// AC	36 at 0.5 A g^{-1}	1 M Na_2SO_4	91.5%, 5000	41.8	200	1
MnO_2//FCO	34 at 0.5 mA cm^{-2}	1 M KOH	112%, 5000	12.36	1739	3
MnO_2@NAC/N AC	75 at 1 A g^{-1}	PVA-KOH	89.5%, 10000	26.7	400	5
AC//$Mn_3(PO_4)_2$ /100mg GF	28 at 0.5 A g^{-1}	6 M KOH	96%, 10000	7.6	360	6
Mn_3O_4//HBC-900	205.7 at 0.5 A g^{-1}	6 M KOH	82.07 %, 10000	43.1	476.2	7
MnHCF//YP-50F	28.1 at 1 A g^{-1}	1 M Na_2SO_4	80.03%, 8000	18.89	981.25	8
MnBPA//AC	**508.8 at 1 mV s^{-1} and 170.6 at 1 A g^{-1}**	**1 M KOH**	**74%, 10000**	**156.6**	**1658**	**This work**

Table S7. Comparison table provided with the energy storage performance of reported manganese-based MSC devices with reference to MnBPA//AC AMSC device

Material	**Areal Capacitance (mF cm^{-2})**	**Electrolyte**	**Stability ,No of cycles**	**Energy density (µWh cm^{-2})**	**Power density (µW cm^{-2})**	**References**
MnO_2 nanoflowers	0.68	PVA/LiCl	>80%, 3000	0.01	1.19	9
NPG/MnO_2 MSC	11.58	PVA/LiCl	80.7%, 5000	0.693	46.3	10
MnO_2@rGO	20.2	PAAK/KOH	No significant decay, 8700	1.01	120	11
VN//MnO2-AMSCs-GE	16.1	5M LiTFSI	90%, 5000	3.5	639	12
rGO//MnO_x-0.9C MSC	1.59	1 M Na_2SO_4	~85%, 1000	0.274	193.6	13
MnBPA//AC MSC	**105.2**	**PVA/KOH**	**91.6%, 5000**	**16.6**	**187.2**	**This work**

References:

1 H. Z. Chi, Y. Q. Wu, Y. K. Shen, C. Zhang, Q. Xiong and H. Qin, *Electrochim. Acta*, 2018, **289**, 158–167.

2 S. Shi, G. Wan, L. Wu, Z. He, K. Wang, Y. Tang, X. Xu and G. Wang, *J. Colloid Interface Sci.*, 2019, **537**, 142–150.

3 P. R. Deshmukh, Y. Sohn and W. G. Shin, *Electrochim. Acta*, 2018, **285**, 381–392.

4 P. Mei, M. Pramanik, C. Young, Z. Huang, M. S. A. Hossain, Y. Sugahara and Y. Yamauchi, *J. Mater. Chem. A*, 2017, **5**, 23259–23266.

5 B. Sun, X. Zhang, X. Fan, R. Wang, H. Bai and X. Wei, *Energy*, 2022, **249**, 123659.

6 A. A. Mirghni, M. J. Madito, T. M. Masikhwa, K. O. Oyedotun, A. Bello and N. Manyala, *J. Colloid Interface Sci.*, 2017, **494**, 325–337.

7 N. C. Horti, A. Samage, M. A. Halakarni, S. K. Chavan, S. R. Inamdar, M. D. Kamatagi and S. K. Nataraj, *Mater. Chem. Phys.*, 2024, **318**, 129276.

8 H. Ju, H. Lang, T. Yi, K. Tian, J. Yue, L. Hu, L. Zhao, S. Liu and D. Kong, *CrystEngComm*, 2024, **26**, 1133–1140.

9 A. Sajedi-Moghaddam, M. Gholami and N. Naseri, *ACS Appl. Mater. Interfaces*, 2023, **15**, 3894–3903.

10 X. Shi, Z. Zeng, C. Liao, S. Tao, E. Guo, X. Long, X. Wang, D. Deng and Y. Dai, *J. Alloys Compd.*, 2018, **739**, 979–986.

11 J. Zhao, Z. Ma, C. Qiao, Y. Fan, X. Qin and G. Shao, *ACS Appl. Mater. Interfaces*, 2022, **14**, 34686–34696.

12 J. Qin, S. Wang, F. Zhou, P. Das, S. Zheng, C. Sun, X. Bao and Z. S. Wu, *Energy Storage Mater.*, 2019, **18**, 397–404.

13 R. Agrawal and C. Wang, *Micromachines*, 2018, **9**, 399.